

# Supporting Information

## Determinants of Catalytic Power and Ligand Binding in Glutamate Racemase

M. Ashley Spies<sup>§,‡,\*</sup>, Joseph G. Reese<sup>§</sup>, Dylan Dodd<sup>¶</sup>, Katherine L. Pankow<sup>§</sup>, Steven R. Blanke<sup>¶,‡</sup> and Jerome Baudry<sup>†</sup>

*Contribution from the <sup>§</sup>Department of Biochemistry, <sup>‡</sup>Institute for Genomic Biology, <sup>¶</sup>Department of Microbiology, University of Illinois, Urbana, Illinois 61801, <sup>†</sup>Department of Biochemistry & Cellular and Molecular Biology, University of Tennessee, Knoxville and Oak Ridge National Laboratories, Center for Molecular Biophysics, Oak Ridge, Tennessee 37830*

### Abbreviations

DAP, diaminopimelate; DPA, dipicolinic acid or 2,6-pyridine dicarboxylic acid; INT, iodonitrotetrazolium chloride; KIE, kinetic isotope effect; LST, linear synchronous transit; MD, molecular dynamics; NAD<sup>+</sup>, nicotinamide adenine dinucleotide; QM/MM, hybrid quantum mechanical-molecular mechanical method;

### Computational

*Parameterization of Glutamate Carbanion.* MMFF94 Force field parameters for the carbanion ligand were obtained from Molecular Operating Environment's (MOE)<sup>1</sup> internal parameter assignment facility, and were modified so that the internal geometry and carbanion/water interaction energies could replicate results from semi-empirical AM1 calculations. **Figure SI-1** shows that the parametrized molecule reproduces the semi-empirical geometry, and **Table S1** indicates that parametrized partial charges can reproduce the carbanion/water interactions energies within 1 kcal/mol of the semi-empirical results, i.e., within 5.5% of the semi-empirical results. In contrast, non-parametrized charges assigned automatically underestimate the strength of the water/carbanion interaction by about 27.5% of the semi-empirical results. AM1-level energy-minimization of the carbanion form of the ligand led to a low energy minimum that exhibits planar C $\alpha$ , C $\beta$ , N and C $\gamma$ (COOH), and a hydrogen-bonding distance between the NH<sub>3</sub> and C $\delta$ 's oxygen, the latter forming a 6-member-like "cyclic" side chain. These structural features of the semi-empirical energy-minimized carbanion differ from the structure of the ligand found in the crystal structure, as shown on **Figure SI-2**. Two dihedral angles determine the internal geometry differences between the two structures: the N/C $\alpha$ /C $\beta$ /C $\gamma$  dihedral angle is of 72.1 degrees in the "non-cyclic" form (from the crystal structure) and of -47.5 degrees in the energy-minimized "cyclic" form.

And the  $C\alpha/C\beta/C\gamma/C\delta$  dihedral is of 59.3 degrees in the “non-cyclic” form (from the crystal structure) and of 83.6 degrees in the energy-minimized “cyclic” structure.

*Classical simulations.* The program Molecular Operating Environment (MOE)<sup>1</sup> from Chemical Computing Group Inc., Montreal, was used for classical simulations. Monomer C from the glutamate racemase (GR) crystal structure (PDB entry 1ZUW)<sup>2</sup> was used to build the model. Residues 255 to 259, missing in the C monomer in the crystal structure, were built using the “homology” facility of MOE while fixing the coordinates of all other atoms. Side-chain orientation of Phe254 (more than 11 Å away from the carbanion’s closest atom) and of His260 were allowed to differ from the crystal structure in order to avoid kinks and/or strains in the protein backbone due to the modeling of the 255/259 region. In the course of subsequent simulations, the side chain of His260 returned to an orientation close to that observed in the crystal structure, while Phe254 in the models stayed oriented toward the surface of the protein, unlike in the crystal structure where it is close to Lys20. No other side chain orientations were significantly affected by of Phe254’s reorientations. Solvent’s oxygen atoms located further than 4.5 Å of any atom of the protein or the ligand were deleted from the model. Hydrogen atoms were added to the model using MOE’s Add Hydrogen facility. Additional water molecules were added using MOE’s Water Soak facility in a 5 Å layer around protein, ligand and crystallographic solvent molecules. The model was then subject to several rounds of energy minimizations. First, all heavy atoms were fixed and energy minimization calculation was run until an energy gradient of 0.05 kcal/mol/Å<sup>2</sup>. Second, all protein backbone atoms were kept fixed and energy minimizations were run until a energy gradient of 0.05 kcal/mol/Å<sup>2</sup>. Finally, all atoms were free to move and energy minimization was run until an energy gradient of 10<sup>-4</sup> kcal/mol/Å<sup>2</sup>. An additional model was built containing the “cyclic” form of the carbanion, i.e., containing the semi-empirical gas phase minimum energy carbanion structure as described below. The “cyclic” ligand was manually inserted in the model, overlapping the C $\alpha$ , C $\beta$ , N and C(backbone carboxyl) atoms. The final energy-minimized structures were used as starting points for Langevin molecular dynamics simulations in the (constant temperature) canonical ensemble for a total simulation time of ~2.3 ns for the model with the “cyclic ligand” and 1.6 ns for the model with the “non-cyclic” ligand at a temperature of 300K using a thermal coupling of 0.1 ps and an integration timestep of 2fs. Snapshots from the molecular dynamics simulation that would minimize the Cys185 sulfur / carbanion C $\alpha$  and/or the Cys74 sulfur / carbanion C $\alpha$  distances are considered as potential good candidates for proton transfer, and were selected for further semi-empirical calculations analysis.

*Semi-empirical Geometry Optimization.* Active site models were constructed by using the coordinates from time points from the selected MD snapshots indicated in Figures 4 and SI-4B, and only keeping atoms that were within 4.5 Å from the atoms of the glutamate carbanion ligand. These models consist of approximately 70 heavy atoms. These structures were used as the initial coordinates for a transition state optimization using the PM3 semi-empirical Hamiltonian implemented in Spartan04<sup>3</sup>. All of the atoms in the model that represent the protein backbone were frozen as well as the atoms of the  $\delta$ -

carboxylate and the  $\gamma$ -carbon of the glutamate carbanion ligand. All structures that converged in the transition state geometry optimization were confirmed to have a single negative eigen value on the Hessian.

*Ab Initio QM/MM Geometry Optimization.*

Two ‘cyclic’ structures, identified by semi-empirical calculations as likely leading to Cys/C $\alpha$  proton transfer, were investigated: one structure was deemed competent for proton transfer between the sulfur of Cys74 and the C $\alpha$  of the glutamate ligand (corresponding the D $\rightarrow$ L-glutamate stereoinversion) and another was for transfer between Cys185 and C $\alpha$  (corresponding to L $\rightarrow$ D-glutamate stereoinversion). Three waters molecules were explicitly included in the QM/MM studies and treated at the MM level in the geometry optimizations with harmonic restraints on their location. All QM/MM geometry optimizations were performed in Qsite 4.0<sup>4</sup>, using HF/6-31G\*\* basis set for the QM portion and OPLS-AA force field for the MM portion. Qsite employs the Frozen Orbital approach to determining QM/MM energies<sup>5-7</sup>. The QM portion consisted of all ligand atoms and the atoms of the side chains of Cys185 and Cys74. For each structure an identical procedure was followed: the structure of the enzyme-glutamate carbanion complex from the MD trajectory (here referred to as the ‘non-minimized enzyme-carbanion complex’) was first energy-minimized, which resulted in transfer of the C $\alpha$  proton to the sulfur atom of either Cys74 or Cys185 (depending on which structure is being considered). This QM/MM minimized structure together with the non-minimized enzyme-carbanion complex were used as input for a Linear Synchronous Transit (LST) transition state geometry optimization, where the initial guess of the transition state is a midpoint (0.5) between reactant and product geometries (placing the proton’s location in the halfway point between the sulfur atom of the Cys residue and the C $\alpha$ ). After 100 iterations, the LST optimization was halted and this structure was used as input for a quasi-Newton transition state geometry optimization until convergence. The structures that converged in the transition state geometry optimization were confirmed to have a single negative eigenvalue on the Hessian.

*High-throughput database virtual screening.* A virtual database (Chemical Computing Group’s Lead-Like Library) containing ~ 1 million compounds was used in virtual high throughput screening experiments. Virtual docking was performed using the program LigandFit<sup>8,9</sup> within the Cerius2 suite (Accelrys, Inc). Energy-minimized structures of the enzyme with either i) cyclic and ii) non-cyclic carbanion substrates were used in the virtual docking. Database’s compounds were protonated, energy minimized, and docked in the binding site, performing *in-situ* ligand conformational search and rigid-body minimization of the docked poses in the protein’s binding site. The docked compounds were scored using the LigScore scoring function available in LigandFit. The docking results were analyzed for biological and computational consistency by i) verifying that the known carbanion ligand was ranked among the best compounds, and ii) verifying that the carbanion was docked in a geometry that reproduces the initial pose.

**Table SI-1 Comparison of Parameterized Glutamate Carbanion to Semi-Empirical AM1 and MMFF94**

calculation	ligand/water interaction energy (kcal/mol)
Semi-empirical	-18.1
Default MMFF	-13.2
Parameterized (AM1)	-19.1

**Table SI-2. Important Changes in Distance that Occur Along the Racemization Reaction Coordinate**

Key *Distances between Heavy Atoms	C chain of PDB 1ZUW	<i>Ab Initio</i> QM/MM Transition State for D-Glu C $\alpha$ Proton Abstraction by Cys74	<i>Ab Initio</i> QM/MM Transition State for L-Glu C $\alpha$ Proton Abstraction by Cyc185
His187( $\delta$ N)- <u><math>\gamma</math>-Carboxylate (OE2)</u>	6.15	2.67	3.43
His187( $\delta$ N)- <u><math>\gamma</math>-Carboxylate (OE1)</u>	6.18	3.75	3.44
Cys74(S)- <u>C<math>\alpha</math></u>	3.46	3.21	3.82
Cys74(S)- <u>NH3+(N)</u>	3.28	3.76	3.59
Cys185(S)- <u>C<math>\alpha</math></u>	4.37	4.25	3.34
Asp(OD1)- <u>NH3+(N)</u>	3.25	4.88	4.60
Asp(OD1)-Wat2(O)	3.70	2.39	2.44
<u><math>\gamma</math>-Carboxylate (OE2)-NH3+</u>	3.83	2.67	2.77
Gly43(N)- <u><math>\gamma</math>-Carboxylate (OE1)</u>	2.83	4.02	4.89
Thr76( $\beta$ -O)- <u><math>\alpha</math>-Carboxylate (OE1)</u>	2.78	5.78	2.69

\*All distances in Å. Bold type face refers to the atoms within the ligand, which may be either in a D-stereoconformation or may have lost its C $\alpha$  proton in a transition state.

**Table SI-3**

Analysis of CD spectra using DICHROWEB				
Protein	% $\alpha$ -helix	% $\beta$ -sheet	% $\beta$ -turn	% unordered
RacE	37 $\pm$ 2	14 $\pm$ 2	20	29 $\pm$ 1
T76A	38 $\pm$ 1	14 $\pm$ 2	20 $\pm$ 1	28 $\pm$ 1

**Table SI-4****Steady State Kinetic Parameters for wt RacE and T76A Mutant**

RacE Species	$k_{cat}$ ( $s^{-1}$ )	$K_M$ (mM)	$k_{cat}/K_M \times (M^{-1} s^{-1})$
Wild-type (D $\rightarrow$ L direction)	1.31 (0.06)	0.25 (0.04)	5.3 (0.8) $\times 10^3$
Wild-type (L $\rightarrow$ D direction)	87 (9)	14 (6)	6 (3) $\times 10^3$
T76A (D $\rightarrow$ L direction)	0.43 (0.05)	8.6 (1.4)	50 (9)

**Table SI-5****Primer Sequences for Cloning and Mutagenesis**

	Primer	Primer sequence 5' $\rightarrow$ 3'
T76A	<i>racE</i> -T76A for <i>racE</i> -T76A rev	5'-GTGATCGCCTGTAATGCAGCAACAGCGATCGC-3' 5'-GCGATCGCTGTTGCTGCATTACAGGCGATCAC-3'
Wild Type (cloning)	<i>racE</i> -WT for <i>racE</i> -WT rev	5'-GCTGCTCGAGTTGTTGGAACAACCAATAGG-3' 5'-AGTGGATCCCTATCTTTTAATCGGTTCTTGC-3'

**Figure SI-1.**

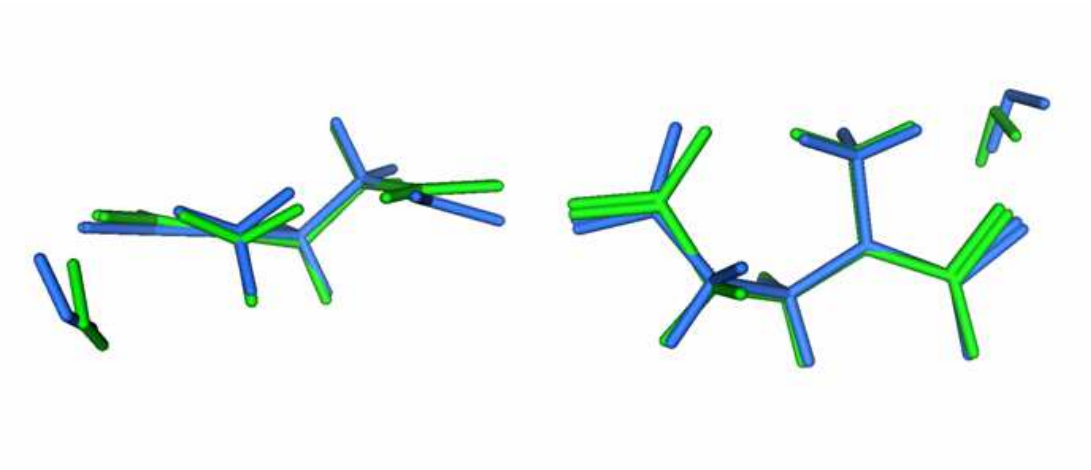


**Figure SI-2A**

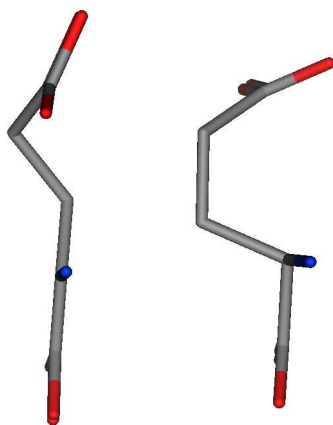


**Figure SI-2B**

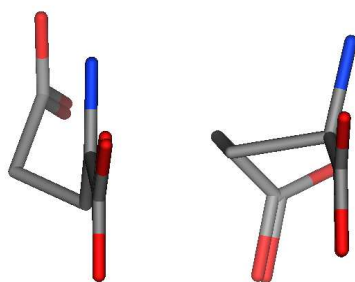


**Figure SI-3**

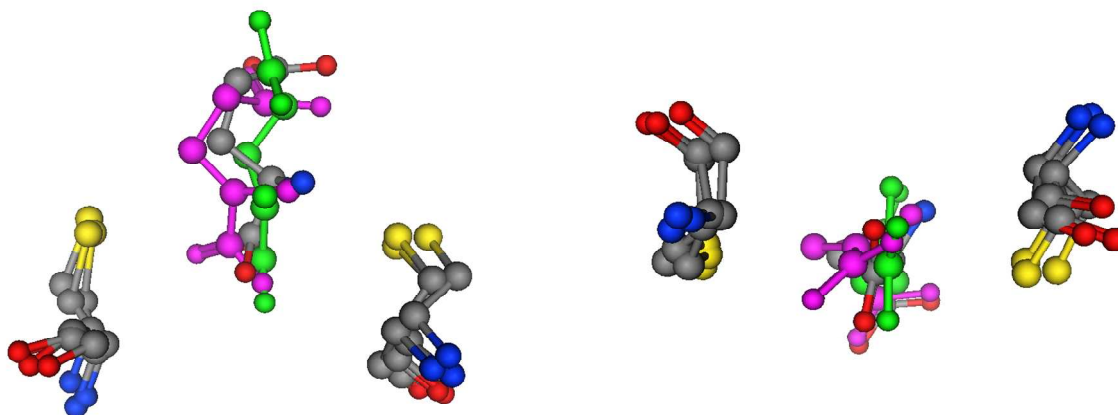




Figure SI-4A

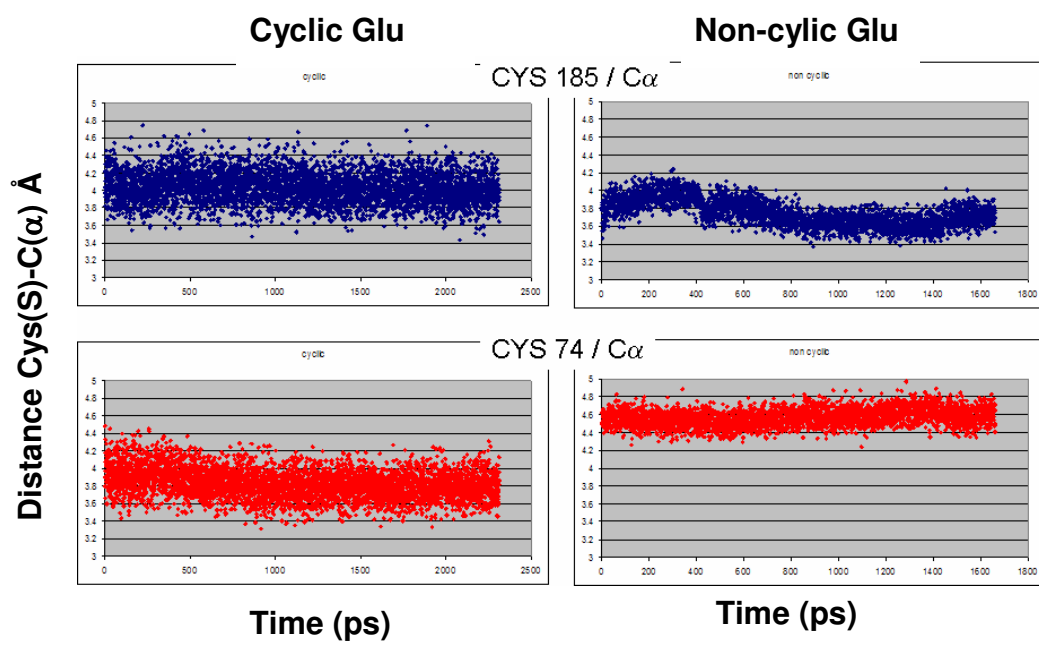
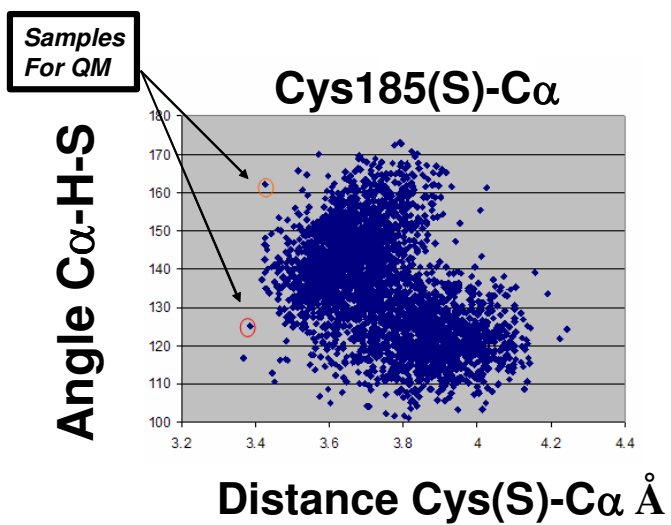
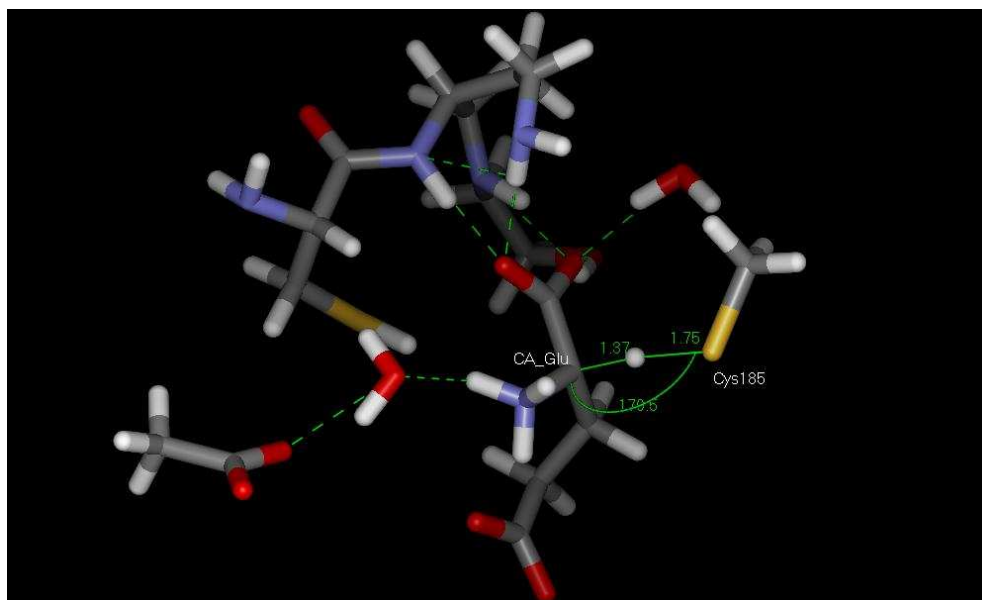


Figure SI-4B



**Figure SI-5A**



**Figure SI-5B**

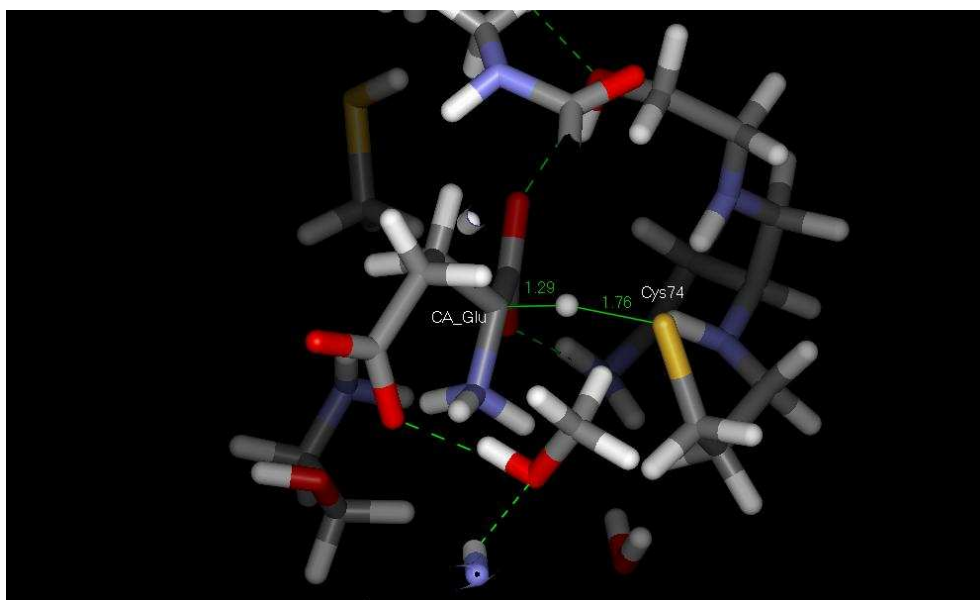


**Figure SI-6A**

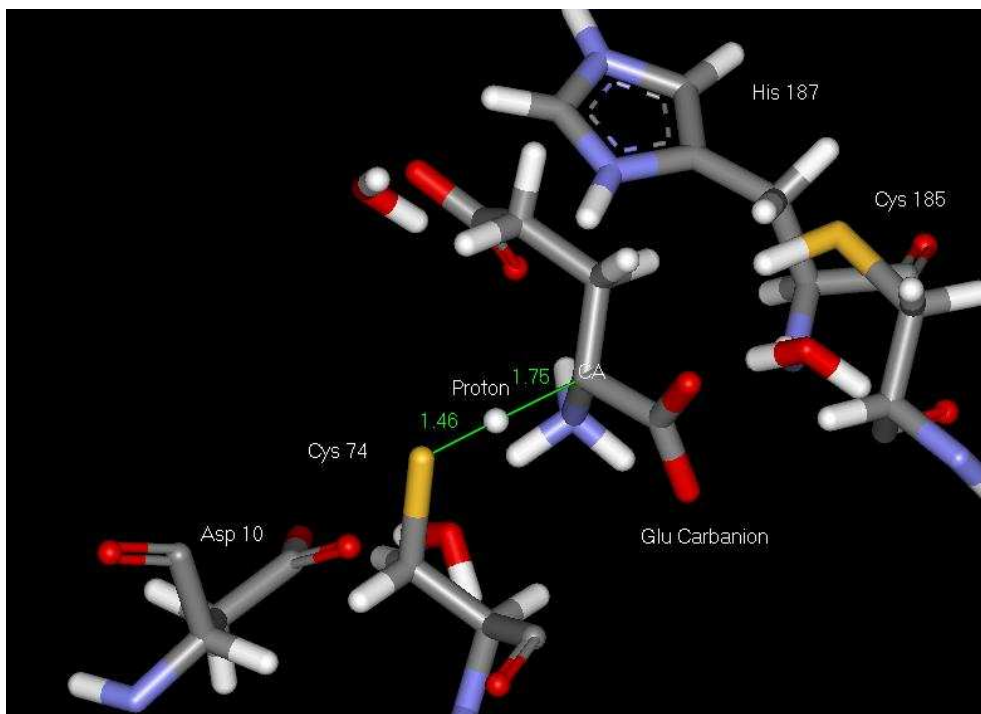


**Figure SI-6B**

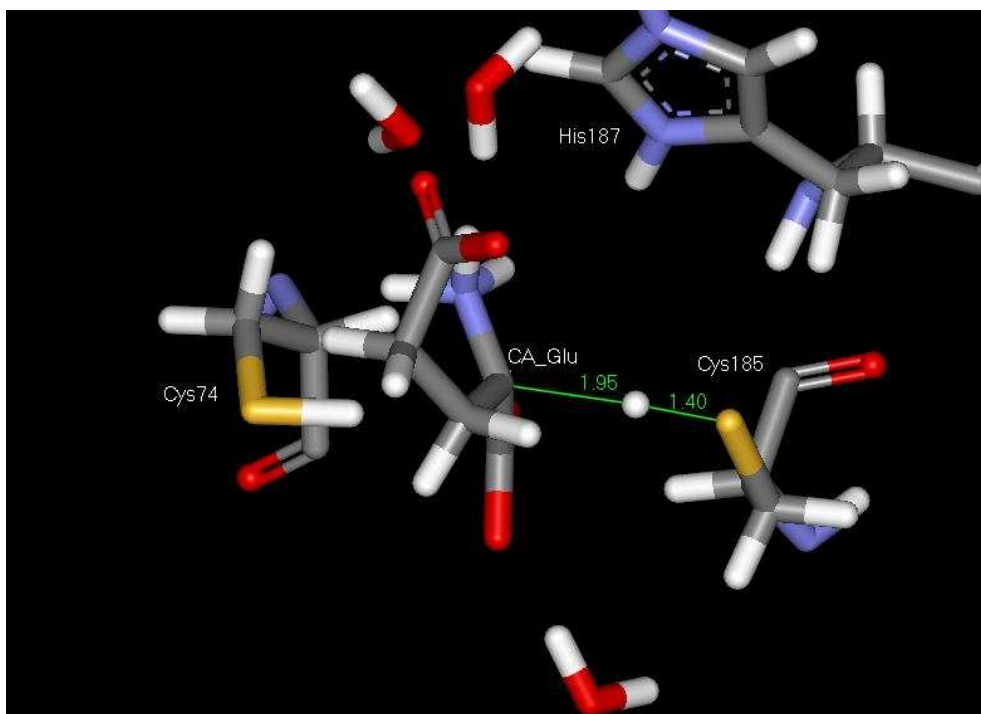


Figure SI-7A

*ab initio* QM/MM Transition State for  
D-Glutamate C $\alpha$  Proton Abstraction

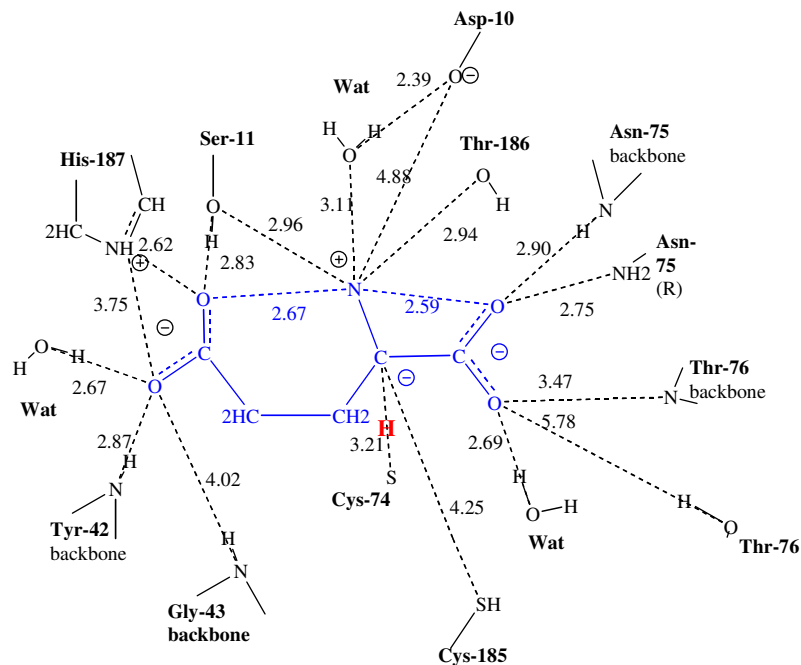
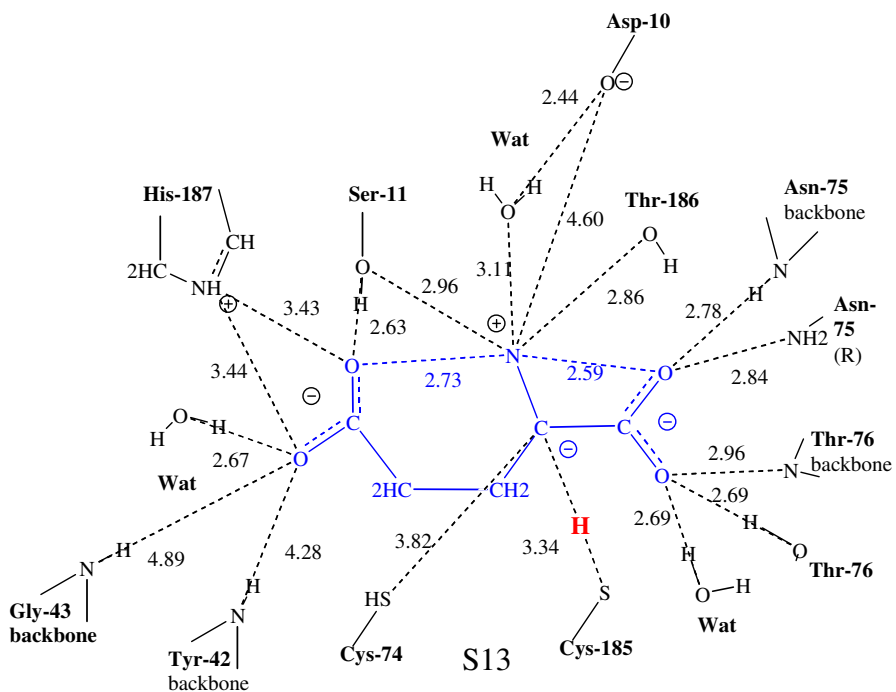
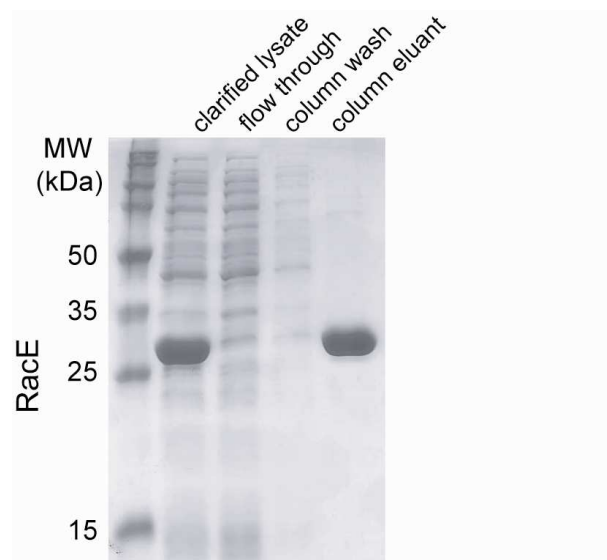


Figure SI-7B

*ab initio* QM/MM Transition State for  
L-Glutamate C $\alpha$  Proton Abstraction



**Figure SI-8**



**Figure SI-9**

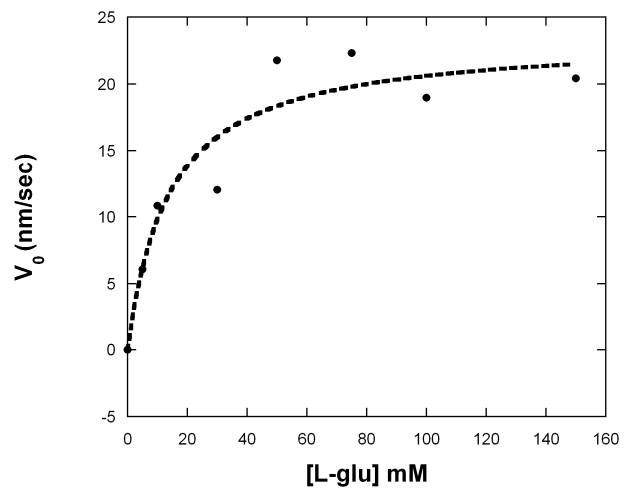


**Figure SI-10 A**

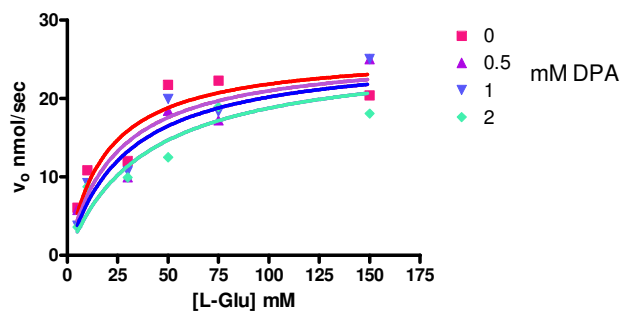
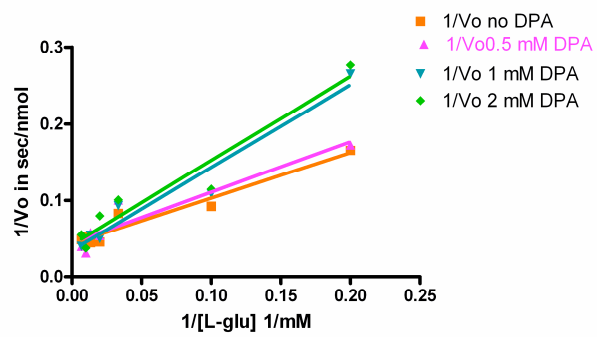


**Figure SI-10 B**





# SI-11

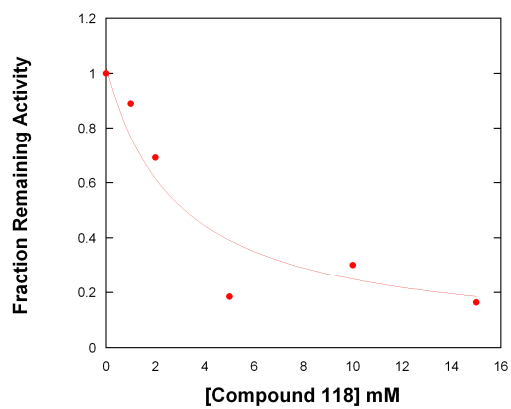


**Figure SI-12A**

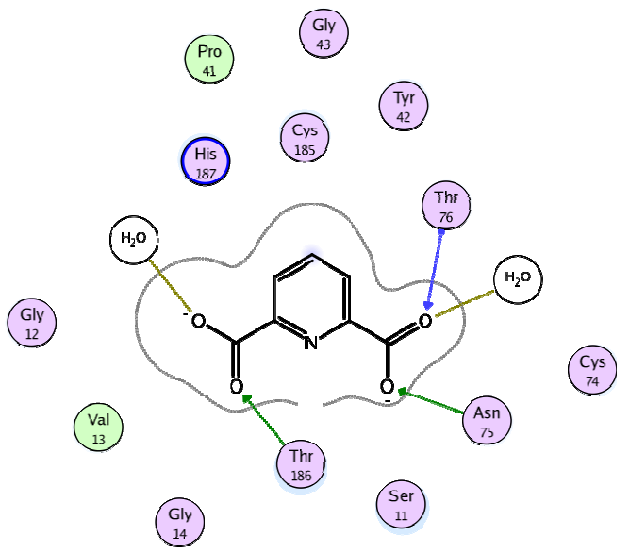
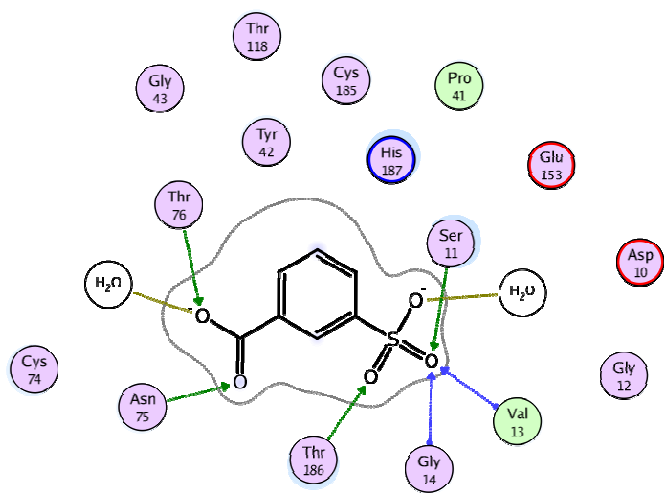


**Figure SI-12B**



- polar
- acidic
- basic
- greasy
- proximity
- contour
- sidechain acceptor
- ← sidechain donor
- backbone acceptor
- ← backbone donor
- solvent residue
- metal complex
- solvent contact
- metal contact
- receptor exposure
- ligand exposure



**Figure SI-1. Energy minimization of parameterized glutamate carbanion with water (MMFF94s) vs semi-empirical (AM1).** The figure shows a superposition of AM1-minimized (blue) and parameterized (green) carbanion/water complexes. The left panel shows a view looking down the  $\alpha$ -NH<sub>3</sub>-C $\alpha$  bond. The right panel is looking down onto the planar C $\alpha$  carbanion.

**Figure SI-2. Comparison of the cyclic (Parameterized) Glutamate Carbanions to D-Glutamate.** Comparison of the energy minimized glutamate carbanion (left) to the D-glutamate from *B. subtilis* glutamate racemase crystal structure (right). **A.** Looking down NH<sub>3</sub>-C $\alpha$  bond. **B.** Looking down  $\alpha$ -carboxylate carbon-C $\alpha$  bond.

**Figure SI-3. Representative Structures Obtained from MD Trajectories; for the cyclic and non-cyclic glutamate carbanion-containing species versus crystal structure.** Superposition of CYS/carbanion/CYS structures: cyclic form of glutamate carbanion shown in green, noncyclic form of glutamate carbanion shown in purple, crystal structure shown in elemental.

**Figure SI-4. Proton Donor-Acceptor Distances from MD.** Distances between proton donor (sulfur atom from Cys catalytic base) and acceptor (C $\alpha$  from cyclic and non-cyclic glutamate carbanion) plotted from MD trajectories. The upper panel shows the Cys185(S)-to-C $\alpha$  distance as a function of time, while the lower panel shows the Cys74(S)-to-C $\alpha$  distance as a function of time. The panels on the left are for the cyclic glutamate carbanion and the panels on the right are for the non-cyclic glutamate carbanion. **B. Identifying Optimal Angles and Distance for Proton Transfer (Non-Cyclic Glutamate Carbanion) from MD Simulations.** A plot of C $\alpha$ -H-S angles and C $\alpha$ -S distances from structures obtained from MD trajectories of the non-cyclic RacE-Glu-carbanion complex. The figure corresponds to coordinates of Cys185. Simulations of the non-cyclic complex did not yield structures where the Cys74-(S) could participate as a proton donor, due to relatively large distance C $\alpha$ -S distances. Structures that yielded angles and distances most appropriate for proton transfer between Cys185 and C $\alpha$  were selected for semi-empirical and *ab initio* transition state geometry optimizations. The specific structures that were selected are circled.

**Figure SI-5. Semi-empirical Transition State Structures.** **A.** Semi-empirical (PM3) transition state for an active site model taken from the MD trajectory (lower panel of Figure 4), for proton transfer between C $\alpha$  of glutamate and Cys185 sulfur atom. **B.** Semi-empirical (PM3) transition state for an active site model taken from the MD trajectory (upper panel of Figure 4), for proton transfer between C $\alpha$  of glutamate and Cys74 sulfur atom. These limited active site models were constructed by using the coordinates from

the MD simulations indicated in Figure 4, and only selecting atoms that were 4.5 Å from the atoms of the glutamate carbanion ligand. These models consist of approximately 70 heavy atoms. The distances between the transferred proton and C $\alpha$  and S atoms, respectively, in the transition states are indicated in green. For more information please see the Computational Procedures section.

**Figure SI-6. *Ab Initio QM/MM Transition State Structures.*** **A.** *ab initio* QM/MM transition state for proton transfer between C $\alpha$  and S of Cys74, obtained from a time point along the MD trajectory (upper panel of Figure 4). **B.** *ab initio* QM/MM transition state for proton transfer between C $\alpha$  and S of Cys185, obtained from a time point along the MD trajectory (lower panel of Figure 4). The *ab initio* portion (6-31G\*\* basis set) for both sections included the Cys side chains and the glutamate carbanion ligand, and the MM portion was the rest of the protein and the 3 local waters. For more details see Computational Procedures section.

**Figure SI-7. *2D Transition State Distance Maps.*** **A.** Active site distances map of the QM/MM transition state for proton transfer in the direction of D $\rightarrow$ L-glutamate racemization (proton transferred between Cys74 sulfur and C $\alpha$  of D-glutamate). **B.** Active site distances map of the QM/MM transition state for proton transfer in the direction of L $\rightarrow$ D-glutamate racemization (proton transferred between Cys185 sulfur and C $\alpha$  of L-glutamate). All distances are in angstroms, and denote the distance between heavy atoms. The ligand is shown in blue and the transferred proton in red. Key distances are summarized in Table SI-2.

**Figure SI-8. *Purification of recombinant RacE.*** The RacE clarified lysate and fractions from nickel-chelate affinity chromatography were analyzed by 12% SDS-PAGE followed by Coomassie brilliant blue G-250 staining. Molecular weight markers appear in the left lane, while fractions from the purification are identified above the gel.

**Figure SI-9. *Steady State Parameters for RacE in the L $\rightarrow$ D Direction.*** The circular dichroism assay was used to follow the conversion of L-glutamate to D-glutamate (assay described in Materials and Methods). The Michaelis-Menten equation was fitted to the data and a  $k_{\text{cat}}$  value of  $87 \pm 9$  s $^{-1}$  and a  $K_M$  value of  $14 \pm 6$  mM was obtained.

**Figure SI-10. *Inhibition of RacE Stereoconversion of Glutamate by DPA in the L $\rightarrow$ D Direction.*** The circular dichroism assay was used to follow the conversion of L-glutamate to D-glutamate (assay described in Materials and Methods). **A.** nonlinear regression global fit of the initial rate kinetic data to Michaelis-Menten equation for competitive inhibition. The fitted  $K_i$  value was  $1.97 \pm 1.16$  mM. Data were collected for DPA concentrations of 0.5, 1 and 2 mM. **B.** shows a Lineweaver-Burk plot of the initial rate kinetic data. The pattern fits a competitive inhibition model, such that all of the

curves converge on a common  $V_{\max}$  value (within error of one another), while there is an increase in the observed  $K_M$  value.

**Figure SI-11. Determination of  $IC_{50}$  Value for Inhibition of RacE Stereoconversion of Glutamate by Compound 118 in the L→D Direction.** The circular dichroism assay was employed (as described in Materials and Methods). A fixed concentration of L-glutamate of 17 mM was used to determine the initial velocity of L→D glutamate stereoconversion in the presence of a fixed concentration of Compound 118. The data were fitted to a standard hyperbolic function for ligand binding. An  $IC_{50}$  value of  $2.9 \pm 1.9$  mM was obtained from the nonlinear regression fit.

**Figure SI-12. Ligand Maps for RacE-DPA and RacE-Compound 118 Complexes** Obtained from *in silico* Screening of the Reactive form of RacE. These complexes were used in the energy correlation graph (Figure 6) of the manuscript. The positioning of these compounds into the active site of the reactive form of RacE is quite similar to one another. Asn75, Thr186 and Thr76 are key hydrogen bond donors in both complexes. A key to the ligand map is presented at the bottom of the figure.

## References Cited in SI

1. Molecular Operating Environment, version 2005-2009; Chemical Computing 2. Ruzhenikov, S. N.; Taal, M. A.; Sedelnikova, S. E.; Baker, P. J.; Rice, D. W., Substrate-induced conformational changes in *Bacillus subtilis* glutamate racemase and their implications for drug discovery. *Structure (Camb)* **2005**, 13, (11), 1707-13.
3. Spartan, version 04/1.0.3; Wavefunction Inc.: Irvine, CA.
4. Q-site version 4.0, Schrodinger, LLC, New York, NY, 2005
5. Murphy, R. B.; Philipp, D. M.; Friesner, R. A., A mixed quantum mechanics/molecular mechanics (QM/MM) method for large-scale modeling of chemistry in protein environments. *Journal of Computational Chemistry* **2000**, 21, (16), 1442-1457.
6. Murphy, R. B.; Philipp, D. M.; Friesner, R. A., Frozen orbital QM/MM methods for density functional theory. *Chemical Physics Letters* **2000**, 321, (1-2), 113-120.
7. Philipp, D. M.; Friesner, R. A., Mixed ab initio QM/MM modeling using frozen orbitals and tests with alanine dipeptide and tetrapeptide. *Journal of Computational Chemistry* **1999**, 20, (14), 1468-1494.
8. Cerius2 LigandFit 4.10, Accelrys, Inc. San Diego, CA.
9. Venkatachalam, C. M.; Jiang, X.; Oldfield, T.; Waldman, M., LigandFit: a novel method for the shape-directed rapid docking of ligands to protein active sites. *J Mol Graph Model* **2003**, 21, (4), 289-307.